Chemical and Process Engineering 2019, 40 (1), 3–19
DOI: 10.24425/cpe.2018.124993

MODELS OF AIRLIFT BIOREACTORS FOR DOUBLE-SUBSTRATE KINETICS. THE ANALYSIS OF SUFFICIENT OXYGENATION CONDITIONS WITH A VIEW OF MATHEMATICAL MODEL CHOICE

Robert Grzywacz*

Cracow University of Technology, Department of Chemical and Process Engineering,
ul. Warszawska 24, 31-155 Cracow, Poland

The quantitative description of an airlift bioreactor, in which aerobic biodegradation limited by carbonaceous substrate and oxygen dissolved in a liquid takes place, is presented. This process is described by the double-substrate kinetics. Mathematical models based on the assumption of plug flow and dispersion flow of liquid through the riser and the downcomer in the reactor were proposed. Calculations were performed for two representative hydrodynamic regimes of reactor operation, i.e. with the presence of gas bubbles only within the riser and for complete gas circulation. The analysis aimed at how the choice of a mathematical model of the process would enable detecting the theoretical occurrence of oxygen deficiency in the airlift reactor. It was demonstrated that the simplification of numerical calculations by assuming the "plug flow" model instead of dispersion with high Péclet numbers posed a risk of improper evaluation of the presence of oxygen deficiency zones. Conclusions related to apparatus modelling and process design were drawn on the basis of the results obtained. The paper is a continuation of an earlier publication (Grzywacz, 2012a) where an analysis of single-substrate models of the airlift reactor was presented.

Keywords: airlift biorector, double-substrate kinetics, modelling, simulation, multiphase bioreactors

1. INTRODUCTION

The airlift reactor is a bubble column apparatus used to conduct many chemical and biochemical processes (Camarasa et al., 2001). Biochemical aerobic processes are especially predestined to be conducted in airlift reactors because of their construction. Despite compact construction, the possibility of conducting simultaneous oxygenation and mixing the reaction medium with bubbling gas is the advantage of airlift reactors. This allows to avoid the destruction of bacteria by mechanical mixers in classic tank reactors.

Apart from problems involving hydrodynamics and mass transfer that are widely described in many papers, from which the most representatives are those written by Gavrilescu and Tudose (1998), Korpijarvi et al. (1999) and Vial et al. (2001), the scientists are also involved in formulating mathematical models and simulation calculations. The examples of published mathematical models of airlift reactor can be found in many papers (Bales and Antosova, 1999; Behin, 2010; Boyadjiev, 2006; Grzywacz, 2012a; Kanai et al., 1996; Kanai et al., 2000; Merchuk and Stein, 1980; Sikula and Markoš, 2008). The majority of the published mathematical models are based on tank-in-series approximation for describing the structure of flowing media or on solving the dispersion model by, e.g. orthogonal collocation. Such an approach to solving

---

* Corresponding author, e-mail: robekk@gmail.com

differential equations results in falsifying results, especially in the area of non-linear analysis (Grzywacz, 2003). Solving balance equations by their direct integration is significantly impeded due to the presence of some hydrodynamic balancing zones in the reactor that result from its characteristic construction. The flow nature of gas and liquid should be defined for each of these zones and the adequate mass balance equations should be formulated. Additionally, two main, from the process point of view, operational states of the reactor can be distinguished. The first one is observed when gas bubbles are present only in the riser, and the second one when gas bubbles are present in each hydrodynamic zone of the reactor. These two operational states are further referred to as hydrodynamic regimes of the reactor operation. If the process occurring in the bioreactor is described by double-substrate kinetics, the number of balance equations is increased by oxygen balances in gas and liquid phases in the specified zones in the reactor. A great number of balance equations also complicates numerical solutions of the mathematical model. In addition, these equations are characterised by a large number of stiffness (Tabiś and Grzywacz, 2011).

This paper presents mathematical models of the heterogeneous airlift bioreactor, in which aerobic biodegradation of carbonaceous substrate with adequately selected bacteria strain takes place. In view of biomass the liquid phase may be treated as pseudohomogenic. The occurring process is described by double-substrate kinetics and can be accomplished in both hydrodynamic regimes defined above. It was demonstrated that despite numerical difficulties it is possible to perform efficient computer simulations for the proposed models using the method of direct integration.

It was analysed how, depending on the mathematical model chosen, the design parameters of the apparatus and the operating conditions affect the oxygenation conditions of the reaction medium. Moreover, both proposed models were demonstrated to predict the appearance of oxygen deficiency zones in different ways. Therefore, it is not possible to substitute the “plug flow” model by the dispersion one if the processes are taking place under conditions characterised by high values of Péclet numbers. This statement can be very important in the design of this type of apparatus.

2. THEORY OF OPERATION AND AIRLIFT REACTOR HYDRODYNAMICS

Due to the nature of media flow through the airlift bioreactor, it can be classified as the loop-type bubble column bioreactor. The recirculation of media in airlift bioreactors can be carried out by a few methods, e.g. by placing a partition in the reactor or introducing a circulation tube. Recirculation can also be provided by a system of two connected tower reactors. One reactor is aerated while the other one operates in the recycling loop. Therefore, there are two fundamental design solutions of the airlift bioreactor. One covers the apparatus with external loop and the second one with internal loop. The conceptual media flow structure scheme in the airlift reactor is presented in Fig. 1.

In both constructional cases, the reactor consists of four hydrodynamic zones: I – riser, II – downcomer, III – degassing zone, IV – demersal zone. Depending on whether gas-liquid mixture undergoes partial or complete degassing in zone III, we can distinguish three hydrodynamic regimes of reactor operation: A – gas phase is present only in the riser, B – the downcomer gradual filling with gas bubbles and C – gas phase circulate between the riser and the downcomer. Full analysis of the work and the hydrodynamics of the reactor airlift has been presented in an earlier publication by Grzywacz (2012a). The hydrodynamic model and its experimental verification are presented elsewhere (Grzywacz, 2008, 2009).

By analysing the reactor operation, it can be said that reactors with internal circulation work mainly in the hydrodynamic regime C, and reactors with external loop operate in the hydrodynamic regime A. Having the above in mind, the reactor operation in two regimes, i.e. regime A and C was analysed in this paper.

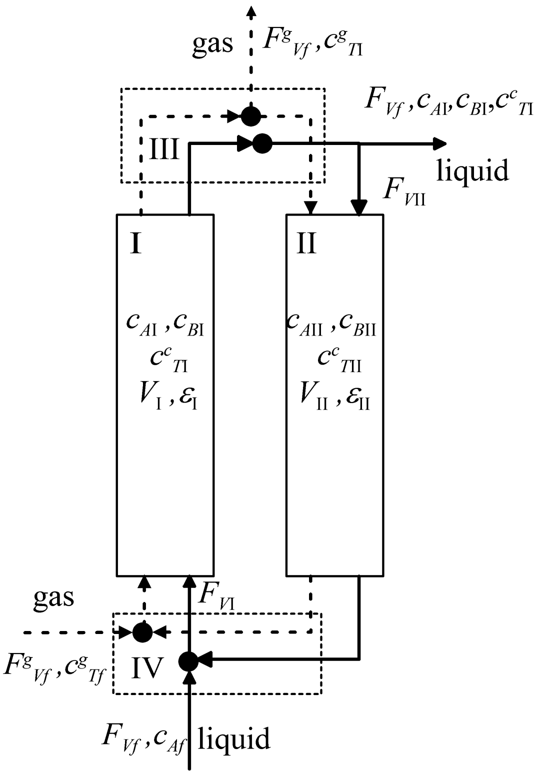

Fig. 1. Schematic diagram of hydrodynamic zone
and media flow structure in airlift bioreactor

2.1. Kinetics of phenol biodegradation

Aerobic biodegradation of phenol by *Pseudomonas Putida* bacteria in the discussed reactor was taken as an example. If the reaction medium is insufficiently oxygenated, then apart from phenol acting as the carbonaceous substrate, oxygen as the extra limiting substrate is required. The uptake rate of carbonaceous substrate r_A, growth rate of biomass r_B and consumption rate of dissolved oxygen r_T are expressed by formulas (1)–(3):

$$r_A\left(c_A, c_B, c_T^c\right) = \frac{1}{w_{BA}} f\left(c_A, c_T^c\right) \cdot c_B \tag{1}$$

$$r_B\left(c_A, c_B, c_T^c\right) = f\left(c_A, c_T^c\right) \cdot c_B \tag{2}$$

$$r_T\left(c_A, c_B, c_T^c\right) = \frac{1}{w_{BT}} f\left(c_A, c_T^c\right) \cdot c_B \tag{3}$$

where function $f(c_A, c_T^c)$ means specific growth rate of microorganisms for the double-substrate kinetics. In this paper, the kinetic model, in which the term related to carbonaceous substrate, was described by the Haldane kinetics and the term related to oxygen was described by the Monod kinetic, was applied to define this value. This model is expressed by the following (4):

$$f\left(c_A, c_T^c\right) = \frac{k \cdot c_A}{K_A + c_A + \dfrac{c_A^2}{K_{in}}} \cdot \frac{c_T^c}{K_T + c_T^c} \tag{4}$$

The following values of kinetic parameters proposed by Seker et al. (1997) were assumed for qualitative analysis: $k = 0.539$ [1/h], $K_A = 0.018539$ [kg/m^3], $K_{in} = 0.099374$ [kg/m^3], $K_T = 0.000048$ [kg/m^3], $w_{BA} = 0.521$ [kgB/kgA], $w_{BT} = 0.338$ [kgB/kgT].

2.2. Mathematic model of the airlift reactor

During the development of bioreactor mathematical model, the adequate number of mathematical equations required for its description should be formulated. The number of these equations depends on the process kinetics and the quantity of zones undergoing balancing.

Biodegradation is conducted in the airlift bioreactor, whose geometry indicates the existence of four already described hydrodynamic zones. For modelling purposes, “plug flow” or dispersion flow of media was assumed in zones I and II. Assuming dispersion flow model allows for testing a wide range of the Péclet number variation. The assumption of the “plug flow” model follows Chisti’s thesis (Chisti, 1989) which says if the Péclet number in the bubble column reactor Pe > 20, then the assumption of the “plug flow” model is acceptable. The substitution of the “plug flow” model for the dispersion one for the high values of the Péclet numbers significantly simplifies numerical calculations (Tabiś and Grzywacz, 2011). The operation of airlift reactor described by the “plug flow” model was formulated in order to verify the assumption following the Chisti’s thesis. For modelling purposes, the zero volumes of zones III and IV were assumed. Zone IV is regarded only as the mixing node. Each model has been considered for two hydrodynamic regimes of reactor operation, i.e. for regime A and C.

To refer to the individual models, i.e. PFM – “plug flow” model for media in zones I and II, ADM – air dispersion model for media flow in zones I and II, appropriate symbols have been introduced. The symbol of hydrodynamic regime for reactor operation is followed by a dash, i.e. A – for the hydrodynamic regime A and C – for the hydrodynamic regime C, respectively.

The following procedure was taken in the formulation of detailed mathematical models. At first, “plug flow” model in zones I and II was discussed. Then, the second, dispersion flow model in zones I and II was discussed. This analysis was conducted first for the hydrodynamic regime A, and then for regime C. Thus it allowed for gradual modification of all formulated equations and stepwise addition of next balance equations in compliance with assumptions related to apparatus structure and operating conditions.

Model No. 1 – **“plug flow”** *in zones I and II, hydrodynamic regime A (PFM–A)*

The mass balance equations of carbonaceous substrate, oxygen and biomass in liquid phase and the equation of oxygen balance in gas phase for the steady state are as follows:

$$u_{c\mathrm{I}}\frac{dc_{A\mathrm{I}}}{dh} = -r_A\left(c_{A\mathrm{I}}, c_{B\mathrm{I}}, c^c_{T\mathrm{I}}\right) \tag{5a}$$

$$u_{c\mathrm{I}}\frac{dc_{B\mathrm{I}}}{dh} = r_B\left(c_{A\mathrm{I}}, c_{B\mathrm{I}}, c^c_{T\mathrm{I}}\right) \tag{5b}$$

$$u_{c\mathrm{I}}\frac{dc^c_{T\mathrm{I}}}{dh} = \frac{ak_{c\mathrm{I}}}{(1-\varepsilon_\mathrm{I})}\left(\frac{c^g_{T\mathrm{I}}}{K_r} - c^c_{T\mathrm{I}}\right) - r_T\left(c_{A\mathrm{I}}, c_{B\mathrm{I}}, c^c_{T\mathrm{I}}\right) \tag{5c}$$

$$u_{g\mathrm{I}}\frac{dc^g_{T\mathrm{I}}}{dh} = -\frac{ak_{c\mathrm{I}}}{\varepsilon_\mathrm{I}}\left(\frac{c^g_{T\mathrm{I}}}{K_r} - c^c_{T\mathrm{I}}\right) \tag{5d}$$

$$u_{c\mathrm{II}}\frac{dc_{A\mathrm{II}}}{dh} = -r_A\left(c_{A\mathrm{II}}, c_{B\mathrm{II}}, c^c_{T\mathrm{II}}\right) \tag{5e}$$

$$u_{c\mathrm{II}}\frac{dc_{B\mathrm{II}}}{dh} = r_B\left(c_{A\mathrm{II}}, c_{B\mathrm{II}}, c^c_{T\mathrm{II}}\right) \tag{5f}$$

$$u_{c\mathrm{II}}\frac{dc^c_{T\mathrm{II}}}{dh} = -r_T\left(c_{A\mathrm{II}}, c_{B\mathrm{II}}, c^c_{T\mathrm{II}}\right) \tag{5g}$$

Equations (5) should be completed with dependences including the presence of mixing node for circulation liquid and fresh raw material (6), i.e.:

$$F_{Vf}^{c} c_{Af} + F_{V\mathrm{II}}^{c} c_{A\mathrm{II}}(H_{\mathrm{II}}) = F_{V\mathrm{I}}^{c} c_{A0} \tag{6a}$$

$$F_{V\mathrm{II}}^{c} c_{B\mathrm{II}}(H_{\mathrm{II}}) = F_{V\mathrm{I}}^{c} c_{B0} \tag{6b}$$

$$F_{Vf}^{c} c_{Tf}^{c} + F_{V\mathrm{II}}^{c} c_{T\mathrm{II}}^{c}(H_{\mathrm{II}}) = F_{V\mathrm{I}}^{c} c_{T0}^{c} \tag{6c}$$

Defining liquid recirculation ratio as $\xi_c = F_{V\mathrm{II}}^{c}/F_{V\mathrm{I}}^{c}$ we obtain the following relationships for the mixing node (7):

$$(1-\xi_c)\, c_{Af} + \xi_c \cdot c_{A\mathrm{II}}(1) = c_{A0} \tag{7a}$$

$$\xi_c \cdot c_{B\mathrm{II}}(1) = c_{B0} \tag{7b}$$

$$(1-\xi_c)\, c_{Tf}^{c} + \xi_c \cdot c_{T\mathrm{II}}^{c}(1) = c_{T0}^{c} \tag{7c}$$

As the riser and downcomer volumes can be different, the coefficient determining zone I volume ratio to the sum of reactor zone I and II volumes was defined $\zeta_{\mathrm{I}} = V_{\mathrm{I}}/\left(V_{\mathrm{I}} + V_{\mathrm{II}}\right)$. Now, the volumes of zone I and II are $V_{\mathrm{I}} = \zeta_{\mathrm{I}} \cdot V$ and $V_{\mathrm{II}} = (1-\zeta_{\mathrm{I}})V$.

Liquid phase residence time in zones I and II can be defined as $\tau_{c\mathrm{I}} = \zeta_{\mathrm{I}} \cdot \tau_c \cdot (1-\varepsilon_{\mathrm{I}}) \cdot (1-\xi_c)$ and $\tau_{c\mathrm{II}} = (1-\zeta_{\mathrm{I}}) \cdot \tau_c \cdot (1-\xi_c)/\xi_c$ where $\tau_c = (V_{\mathrm{I}} + V_{\mathrm{II}})/F_{Vf}^{c}$.

The expression defining gas residence time in zone I should also be defined. This value can be determined from the following dependence: $\tau_{g\mathrm{I}} = \zeta_{\mathrm{I}} \cdot \tau_g \cdot \varepsilon_{\mathrm{I}}$ where $\tau_g = (V_{\mathrm{I}} + V_{\mathrm{II}})/F_{Vf}^{g}$.

Now, the dependence for determining liquid recirculation ratio ξ_c is to be defined. According to the formula of $\xi_c = F_{V\mathrm{II}}^{c}/F_{V\mathrm{I}}^{c}$ and after determining liquid velocity in zones I and II from the hydrodynamic model, it can be expressed as: $\xi_c = u_{c\mathrm{II}}\,(1-\varepsilon_{\mathrm{II}})\,(1-\zeta_{\mathrm{I}}) / \left(u_{c\mathrm{I}}\,(1-\varepsilon_{\mathrm{I}})\,\zeta_{\mathrm{I}}\right)$.

Dimensionless state variables are introduced for further analysis. They are: degree of conversion of carbonaceous substrate, α, dimensionless concentration of biomass, β, dimensionless concentration of oxygen dissolved in liquid, γ, and dimensionless concentration of oxygen in gas phase, δ, defined as: $\alpha_i = \left(c_{Af} - c_{Ai}\right)/c_{Af}$; $\beta_i = c_{Bi}/c_{Af}$; $\gamma_i = c_T^c/c_{Af}$ and $\delta_i = c_T^g/c_{Tf}^g$, where $i = \mathrm{I}, \mathrm{II}$, respectively.

By introducing the above-defined dimensionless state variables α, β, γ and δ, and the model parameters and the reactor dimensionless length $z = h/H$ to Eqs. (5), a system of seven differential Eqs. (8) with boundary conditions defined for $z = 0$ and $z = 1$ (9) can be obtained.

$$\frac{d\alpha_{\mathrm{I}}}{dz} = \tau_{c\mathrm{I}} r_A\left(\alpha_{\mathrm{I}}, \beta_{\mathrm{I}}, \gamma_{\mathrm{I}}\right) \tag{8a}$$

$$\frac{d\beta_{\mathrm{I}}}{dz} = \tau_{c\mathrm{I}} r_B\left(\alpha_{\mathrm{I}}, \beta_{\mathrm{I}}, \gamma_{\mathrm{I}}\right) \tag{8b}$$

$$\frac{d\gamma_{\mathrm{I}}}{dz} = \frac{\tau_{c\mathrm{I}} a k_{c\mathrm{I}}}{(1-\varepsilon_{\mathrm{I}})}\left(\frac{c_{Tf}^{g}}{c_{Af} K_r}\delta_{\mathrm{I}} - \gamma_{\mathrm{I}}\right) - \tau_{c\mathrm{I}} r_T\left(\alpha_{\mathrm{I}}, \beta_{\mathrm{I}}, \gamma_{\mathrm{I}}\right) \tag{8c}$$

$$\frac{d\delta_{\mathrm{I}}}{dz} = -\frac{\tau_{g\mathrm{I}} a k_{c\mathrm{I}}}{\varepsilon_{\mathrm{I}}} \cdot \frac{c_{Af}}{c_{Tf}^{g}}\left(\frac{c_{Tf}^{g}}{c_{Af} K_r}\delta_{\mathrm{I}} - \gamma_{\mathrm{I}}\right) \tag{8d}$$

$$\frac{d\alpha_{\mathrm{II}}}{dz} = \tau_{c\mathrm{II}} r_A\left(\alpha_{\mathrm{II}}, \beta_{\mathrm{II}}, \gamma_{\mathrm{II}}\right) \tag{8e}$$

$$\frac{d\beta_{\mathrm{II}}}{dz} = \tau_{c\mathrm{II}} r_B\left(\alpha_{\mathrm{II}}, \beta_{\mathrm{II}}, \gamma_{\mathrm{II}}\right) \tag{8f}$$

$$\frac{d\gamma_{\mathrm{II}}}{dz} = \tau_{c\mathrm{II}} r_T \left(\alpha_{\mathrm{II}}, \beta_{\mathrm{II}}, \gamma_{\mathrm{II}}\right) \tag{8g}$$

$$\alpha_{\mathrm{I}}(0) = \alpha_0\,; \qquad \beta_{\mathrm{I}}(0) = \beta_0\,; \qquad \gamma_{\mathrm{I}}(0) = \gamma_0\,; \qquad \delta_{\mathrm{I}}(0) = 1 \tag{9a}$$

$$\alpha_{\mathrm{II}}(0) = \alpha_{\mathrm{I}}(1)\,; \qquad \beta_{\mathrm{II}}(0) = \beta_{\mathrm{I}}(1)\,; \qquad \gamma_{\mathrm{II}}(0) = \gamma_{\mathrm{I}}(1) \tag{9b}$$

along with the algebraic Eqs. (10) characterising the mixing node:

$$\alpha_0 - \xi_c \alpha_{\mathrm{II}}(1) = 0 \tag{10a}$$

$$\xi_c \beta_{\mathrm{II}}(1) - \beta_0 = 0 \tag{10b}$$

$$\gamma_0 - \xi_c \gamma_{\mathrm{II}}(1) - (1 - \xi_c)\,\gamma_f = 0 \tag{10c}$$

Model No. 2 – in zones I and II, hydrodynamic regime C (PFM–C)

In hydrodynamic regime C, gas bubbles are present also in zone II. Model No. 1 was modified by formulating oxygen balance equation in gas phase in zone II. The oxygen balance equation in liquid phase in zone II should also include oxygen mass transfer from gas phase to liquid one. Then, the extra equation in the mixing node, related to gas phase circulation, appears.

Considering the above, the Eqs. (5a)–(5d) and (8a)–(8d) for zone I demonstrate no changes. Also, some equations for zone II, namely (5e, f) and (8e, f), would be identical. Equation (5g), that includes oxygen mass transfer from the gas phase to the liquid one, would be as follows:

$$u_{c\mathrm{II}} \frac{dc^c_{T\mathrm{II}}}{dh} = \frac{ak_{c\mathrm{II}}}{(1 - \varepsilon_{\mathrm{II}})} \left(\frac{c^g_{T\mathrm{II}}}{K_r} - c^c_{T\mathrm{II}} \right) - r_T \left(c_{A\mathrm{II}}, c_{B\mathrm{II}}, c^c_{T\mathrm{II}} \right) \tag{11a}$$

Also, the equation of oxygen balance in the gas phase in zone II should be formulated. This is expressed by:

$$u_{g\mathrm{II}} \frac{dc^g_{T\mathrm{II}}}{dh} = -\frac{ak_{c\mathrm{II}}}{\varepsilon_{\mathrm{II}}} \left(\frac{c^g_{T\mathrm{II}}}{K_r} - c^c_{T\mathrm{II}} \right) \tag{11b}$$

After introducing previously defined dimensionless values α, β, γ, δ and z into Eqs. (11), we obtain Eqs. (12):

$$\frac{d\gamma_{\mathrm{II}}}{dz} = \frac{\tau_{c\mathrm{II}} ak_{c\mathrm{II}}}{(1 - \varepsilon_{\mathrm{II}})} \left(\frac{c^g_{Tf}}{c_{Af} K_r} \delta_{\mathrm{II}} - \gamma_{\mathrm{II}} \right) - \tau_{c\mathrm{II}} r_T \left(\alpha_{\mathrm{II}}, \beta_{\mathrm{II}}, \gamma_{\mathrm{II}}\right) \tag{12a}$$

$$\frac{d\delta_{\mathrm{II}}}{dz} = -\frac{\tau_{g\mathrm{II}} ak_{c\mathrm{II}}}{\varepsilon_{\mathrm{II}}} \cdot \frac{c_{Af}}{c^g_{Tf}} \left(\frac{c^g_{Tf}}{c_{Af} K_r} \delta_{\mathrm{II}} - \gamma_{\mathrm{II}} \right) \tag{12b}$$

Some initial conditions related to these equations are slightly changed. Particularly, the condition $\delta_{\mathrm{I}}(0) = 1$ is expressed as $\delta_{\mathrm{I}}(0) = \delta_0$. Also, the initial condition for Eq. (12b) should be formulated. This is expressed by the following equality: $\delta_{\mathrm{II}}(0) = \delta_{\mathrm{I}}(1)$.

Gas recirculation ratio, similarly to the liquid recirculation ratio should be introduced. This is expressed by $\xi_g = F^{\mathrm{g}}_{V\mathrm{II}} / F^{\mathrm{g}}_{V\mathrm{I}}$. Considering the above remarks, a dependence defining gas behaviour in the mixing node looks as follows: $\delta_0 - \xi_g \delta_{\mathrm{II}}(1) - (1 - \xi_g) = 0$.

Due to gas presence in zone II, the expression of liquid residence time in zone II was modified to the following form: $\tau_{c\mathrm{II}} = \tau_c (1 - \zeta_{\mathrm{I}})(1 - \varepsilon_{\mathrm{II}})(1 - \xi_c)/\xi_c$.

Similarly, the expression defining gas phase residence time in zone II is changed into $\tau_{g\mathrm{II}} = (1 - \zeta_{\mathrm{I}}) \cdot \tau_g \cdot \varepsilon_{\mathrm{II}} \left(1 - \xi_g\right) / \xi_g$.

Now, a dependence for determining gas recirculation ratio ξ_g remains to be defined. According to the definition of ξ_g, and after determining gas velocity in zones I and II from the hydrodynamic model it can be described by $\xi_g = u_{g\mathrm{II}}\varepsilon_{\mathrm{II}}(1-\zeta_{\mathrm{I}})/\left(u_{g\mathrm{I}}\varepsilon_{\mathrm{II}}\zeta_{\mathrm{I}}\right)$.

Then, the way of developing models for dispersion flow in zone I and II is presented. As previously, the formulation of models should start from the process which occurs in the hydrodynamic regime A. This allows for introducing required modification for the process occurring in the hydrodynamic regime C. The dispersion flow is assumed for both phases present in the bioreactor.

Model No. 3 – dispersion flow in zones I and II, hydrodynamic regime A (ADM–A)

The mass balance equations of carbonaceous substrate A, biomass B and oxygen T in liquid phase for the assumed flow have the following form (13):

$$D^c_{m\mathrm{I}}\frac{d^2c_{A\mathrm{I}}}{dh^2} - u_{c\mathrm{I}}\frac{dc_{A\mathrm{I}}}{dh} - r_A\left(c_{A\mathrm{I}}, c_{B\mathrm{I}}, c^c_{T\mathrm{I}}\right) = 0 \tag{13a}$$

$$D^c_{m\mathrm{I}}\frac{d^2c_{B\mathrm{I}}}{dh^2} - u_{c\mathrm{I}}\frac{dc_{B\mathrm{I}}}{dh} + r_B\left(c_{A\mathrm{I}}, c_{B\mathrm{I}}, c^c_{T\mathrm{I}}\right) = 0 \tag{13b}$$

$$D^c_{m\mathrm{I}}\frac{d^2c^{\mathrm{c}}_{T\mathrm{I}}}{dh^2} - u_{c\mathrm{I}}\frac{dc^c_{T\mathrm{I}}}{dh} - r_T\left(c_{A\mathrm{I}}, c_{B\mathrm{I}}, c^c_{T\mathrm{I}}\right) + \frac{ak_{c\mathrm{I}}}{(1-\varepsilon_{\mathrm{I}})}\left(\frac{c^g_{T\mathrm{I}}}{K_r} - c^c_{T\mathrm{I}}\right) = 0 \tag{13c}$$

$$D^g_{m\mathrm{I}}\frac{d^2c^g_{T\mathrm{I}}}{dh^2} - u_{g\mathrm{I}}\frac{dc^g_{T\mathrm{I}}}{dh} - \frac{ak_{c\mathrm{I}}}{\varepsilon_{\mathrm{I}}}\left(\frac{c^g_{T\mathrm{I}}}{K_r} - c^c_{T\mathrm{I}}\right) = 0 \tag{13d}$$

$$D^c_{m\mathrm{II}}\frac{d^2c_{A\mathrm{II}}}{dh^2} - u_{c\mathrm{II}}\frac{dc_{A\mathrm{II}}}{dh} - r_A\left(c_{A\mathrm{II}}, c_{B\mathrm{II}}, c^c_{T\mathrm{II}}\right) = 0 \tag{13e}$$

$$D^c_{m\mathrm{II}}\frac{d^2c_{B\mathrm{II}}}{dh^2} - u_{c\mathrm{II}}\frac{dc_{B\mathrm{II}}}{dh} + r_B\left(c_{A\mathrm{II}}, c_{B\mathrm{II}}, c^c_{T\mathrm{II}}\right) = 0 \tag{13f}$$

$$D^c_{m\mathrm{II}}\frac{d^2c_{T\mathrm{II}}}{dh^2} - u_{c\mathrm{II}}\frac{dc_{T\mathrm{II}}}{dh} - r_T\left(c_{A\mathrm{II}}, c_{B\mathrm{II}}, c^c_{T\mathrm{II}}\right) = 0 \tag{13g}$$

The mixing node equations are identical with Eq. (7).

After introducing previously defined dimensionless values to Eqs. (13), the following forms of model equations are obtained:

$$\frac{1}{\mathrm{Pe}_{c\mathrm{I}}}\frac{d^2\alpha_{\mathrm{I}}}{dz^2} - \frac{d\alpha_{\mathrm{I}}}{dz} + \tau_{c\mathrm{I}}r_B\left(\alpha_{\mathrm{I}}, \beta_{\mathrm{I}}, \gamma_{\mathrm{I}}\right) = 0 \tag{14a}$$

$$\frac{1}{\mathrm{Pe}_{c\mathrm{I}}}\frac{d^2\beta_{\mathrm{I}}}{dz^2} - \frac{d\beta_{\mathrm{I}}}{dz} + \tau_{c\mathrm{I}}r_B\left(\alpha_{\mathrm{I}}, \beta_{\mathrm{I}}, \gamma_{\mathrm{I}}\right) = 0 \tag{14b}$$

$$\frac{1}{\mathrm{Pe}_{c\mathrm{I}}}\frac{d^2\gamma_{\mathrm{I}}}{dz^2} - \frac{d\gamma_{\mathrm{I}}}{dz} - \tau_{c\mathrm{I}}r_T\left(\alpha_{\mathrm{I}}, \beta_{\mathrm{I}}, \gamma_{\mathrm{I}}\right) + \frac{\tau_{c\mathrm{I}}ak_{c\mathrm{I}}}{(1-\varepsilon_{\mathrm{I}})}\left(\frac{c^g_{Tf}}{c_{Af}K_r}\delta_{\mathrm{I}} - \gamma_{\mathrm{I}}\right) = 0 \tag{14c}$$

$$\frac{1}{\mathrm{Pe}_{g\mathrm{I}}}\frac{d^2\delta_{\mathrm{I}}}{dz^2} - \frac{d\delta_{\mathrm{I}}}{dz} - \frac{\tau_{c\mathrm{I}}ak_{c\mathrm{I}}}{\varepsilon_{\mathrm{I}}}\cdot\frac{c_{Af}}{c^g_{tf}}\left(\frac{c^g_{Tf}}{c_{Af}K_r}\delta_{\mathrm{I}} - \gamma_{\mathrm{I}}\right) = 0 \tag{14d}$$

$$\frac{1}{\mathrm{Pe}_{c\mathrm{II}}}\frac{d^2\alpha_{\mathrm{II}}}{dz^2} - \frac{d\alpha_{\mathrm{II}}}{dz} + \tau_{c\mathrm{II}}r_B\left(\alpha_{\mathrm{II}}, \beta_{\mathrm{II}}, \gamma_{\mathrm{II}}\right) = 0 \tag{14e}$$

$$\frac{1}{\mathrm{Pe}_{c\mathrm{II}}}\frac{d^2\beta_{\mathrm{II}}}{dz^2}-\frac{d\beta_{\mathrm{II}}}{dz}+\tau_{c\mathrm{II}}r_B\left(\alpha_{\mathrm{II}},\beta_{\mathrm{II}},\gamma_{\mathrm{II}}\right)=0 \tag{14f}$$

$$\frac{1}{\mathrm{Pe}_{c\mathrm{II}}}\frac{d^2\gamma_{\mathrm{II}}}{dz^2}-\frac{d\gamma_{\mathrm{II}}}{dz}-\tau_{c\mathrm{II}}r_T\left(\alpha_{\mathrm{II}},\beta_{\mathrm{II}},\gamma_{\mathrm{II}}\right)=0 \tag{14g}$$

where Pe is the Péclet number defined as $\mathrm{Pe} = uH/D_m$.

The mixing node equations are identical with Eqs. (10).

The formulation of adequate boundary conditions is required for solving the above system of equations. For zone I, they have the following form (15):

$$\frac{1}{\mathrm{Pe}_{c\mathrm{I}}}\frac{d\alpha_{\mathrm{I}}(0)}{dh}-\alpha_{\mathrm{I}}(0)+\alpha_0=0 \tag{15a}$$

$$\frac{1}{\mathrm{Pe}_{c\mathrm{I}}}\frac{d\beta_{\mathrm{I}}(0)}{dh}-\beta_{\mathrm{I}}(0)+\beta_0=0 \tag{15b}$$

$$\frac{1}{\mathrm{Pe}_{c\mathrm{I}}}\frac{d\gamma_{\mathrm{I}}(0)}{dh}-\gamma_{\mathrm{I}}(0)+\gamma_0=0 \tag{15c}$$

$$\frac{1}{\mathrm{Pe}_{g\mathrm{I}}}\frac{d\delta_{\mathrm{I}}(0)}{dh}-\delta_{\mathrm{I}}(0)+1=0 \tag{15d}$$

$$\frac{d\alpha_{\mathrm{I}}(1)}{dz}=0 \tag{15e}$$

$$\frac{d\beta_{\mathrm{I}}(1)}{dz}=0 \tag{15f}$$

$$\frac{d\gamma_{\mathrm{I}}(1)}{dz}=0 \tag{15g}$$

$$\frac{d\delta_{\mathrm{I}}(1)}{dz}=0 \tag{15h}$$

whereas for zone II (16):

$$\frac{1}{\mathrm{Pe}_{c\mathrm{II}}}\frac{d\alpha_{\mathrm{II}}(0)}{dh}-\alpha_{\mathrm{II}}(0)+\alpha_{\mathrm{I}}(1)=0 \tag{16a}$$

$$\frac{1}{\mathrm{Pe}_{c\mathrm{II}}}\frac{d\beta_{\mathrm{II}}(0)}{dh}-\beta_{\mathrm{II}}(0)+\beta_{\mathrm{I}}(1)=0 \tag{16b}$$

$$\frac{1}{\mathrm{Pe}_{c\mathrm{II}}}\frac{d\gamma_{\mathrm{II}}(0)}{dh}-\gamma_{\mathrm{II}}(0)+\gamma_{\mathrm{I}}(1)=0 \tag{16c}$$

$$\frac{d\alpha_{\mathrm{II}}(1)}{dz}=0 \tag{16d}$$

$$\frac{d\beta_{\mathrm{II}}(1)}{dz}=0 \tag{16e}$$

$$\frac{d\gamma_{\mathrm{II}}(1)}{dz}=0 \tag{16f}$$

The other parameters of the model are defined as for model No. 1.

Model No. 4 – dispersion flow in zones I and II, hydrodynamic regime C (ADM–C)

For the analysed model, the change of the hydrodynamic regime A into C requires the model to be completed similar to model No. 2 during its formulation. Only the final forms of the equations and dependences are presented here. The sequence of their introduction is identical with that of model No. 2.

Equations (14a)–(14f) are identical both for model No. 3 and model No. 4. The final form of Eq. (14g) is:

$$\frac{1}{\mathrm{Pe}_{c\mathrm{II}}}\frac{d^2\gamma_{\mathrm{II}}}{dz^2}-\frac{d\gamma_{\mathrm{II}}}{dz}-\tau_{c\mathrm{II}}r_T\left(\alpha_{\mathrm{II}},\beta_{\mathrm{II}},\gamma_{\mathrm{II}}\right)+\frac{\tau_{c\mathrm{II}}ak_{c\mathrm{II}}}{(1-\varepsilon_{\mathrm{II}})}\left(\frac{c^g_{Tf}}{c_{Af}K_r}\delta_{\mathrm{II}}-\gamma_{\mathrm{II}}\right)=0 \tag{17a}$$

while the final form of the equation defining oxygen balance in gas phase for zone II is as follows:

$$\frac{1}{\mathrm{Pe}_{c\mathrm{II}}}\frac{d^2\gamma_{\mathrm{II}}}{dz^2}-\frac{d\gamma_{\mathrm{II}}}{dz}-\frac{\tau_{g\mathrm{II}}ak_{c\mathrm{II}}}{\varepsilon_{\mathrm{II}}}\cdot\frac{c_{Af}}{c^g_{Tf}}\left(\frac{c^g_{Tf}}{c_{Af}K_r}\delta_{\mathrm{II}}-\gamma_{\mathrm{II}}\right)=0 \tag{17b}$$

The modification of the boundary condition (15d) to the form (18a) is the next step:

$$\frac{1}{\mathrm{Pe}_{g\mathrm{I}}}\frac{d\delta_{\mathrm{I}}(0)}{dh}-\delta_{\mathrm{I}}(0)+\delta_0=0 \tag{18a}$$

Then, the conditions are to be added to Eq. (17b), i.e.:

$$\frac{1}{\mathrm{Pe}_{g\mathrm{II}}}\frac{d\delta_{\mathrm{II}}(0)}{dh}-\delta_{\mathrm{II}}(0)+\delta_{\mathrm{I}}(1)=0 \tag{18b}$$

$$\frac{d\delta_{\mathrm{II}}(1)}{dz}=0 \tag{18c}$$

The other dependences and expressions present in the model discussed are defined identically as for model No. 2.

Oxygen gas-liquid equilibrium constant K_r, which is present in the equations of discussed mathematical models, following Wisecarver and Fan (1989) is assumed to equal 30 [$\mathrm{m}^3_{\mathrm{liquid}}/\mathrm{m}^3_{\mathrm{air}}$]. The procedure proposed by Chisti (Chisti, 1989) was applied in order to calculate mass transfer coefficient in zones I and II. In this method, mean oxygen volumetric mass transfer coefficient is determined according to the following formula: $ak_c = 1.27\times10^{-4}(P_g/V)$ where $(P_g/V) = \rho_c\cdot g\cdot u_{0g}/(1+S_{\mathrm{II}}/S_{\mathrm{I}})$. However, the zonal volumetric oxygen transfer coefficients in this system are determined from Eqs. (19):

$$ak_c=\frac{ak_{c\mathrm{I}}S_{\mathrm{I}}+ak_{c\mathrm{II}}S_{\mathrm{II}}}{S_{\mathrm{I}}+S_{\mathrm{II}}} \tag{19a}$$

$$ak_{c\mathrm{II}}=\Psi\cdot ak_{c\mathrm{I}} \tag{19b}$$

The value of Ψ coefficient is 0.8, as recommended by Chisti.

The value of coefficient of liquid axial dispersion $D^c_{m\mathrm{I}}$, which is required to determine the Péclet number for liquid in zone I, is determined from the dependence proposed by Towell and Ackermann (1972) $D^c_{m\mathrm{I}} = 2.61 d_{\mathrm{I}}^{1.5} u_{0g}^{0.5}$. The Péclet number for liquid in zone II was assumed to be a two-fold value of that number for liquid in zone I.

The Péclet number for gas in zones I and II is the last parameter of the model. Its values were determined from a dependence proposed by Sanchez et al. (2004): $\mathrm{Pe}_{gi} = 8.28\left(\mathrm{Fr}_{gi}^{1/3}\right)^{1.364}\cdot(H/d_i)$ where: $\mathrm{Fr}_{gi} = u_{gi}/\sqrt{g\cdot d_i}$ and $i = \mathrm{I}, \mathrm{II}$.

The mathematical models presented above are the base for analysing airlift bioreactor operation under defined hydrodynamic conditions, i.e. in the hydrodynamic regime A or C, and for the assumed structure of the media flow, i.e. for plug or dispersion flows, respectively. The relevant boundary value problem was solved in order to obtain distributions of carbonaceous substrate conversion degree and biomass and oxygen dimensionless concentration as the function of reactor length. Differential equations were integrated by the fourth order Runge–Kutty method. The Newton algorithm was used to fit boundary conditions between the reactor zones.

All calculations for simulations presented below were carried out for the values of process parameters that corresponded to stable steady states. The parameter values were chosen to maximise the effect of oxygen deficiency. Non-linear analysis of steady states has been presented elsewhere (Grzywacz, 2012b).

The calculations were performed for selected process parameters. These are as follows: mass concentration of carbonaceous substrate in the feed stream, c_{Af}, gas mean residence time in the reactor, τ_g, and liquid mean residence time in the reactor, τ_c, respectively. Analysing the branches of steady states, the value of one of the above parameters was chosen. The values of the other process parameters result directly from the parameters of the operating point of the reactor selected on the branch of steady states. The diameters of riser and downcomer, expressed by the volume distribution coefficient ζ, were the analysed construction parameters. Its values were also chosen in the manner described above. The other hydrodynamic and process parameters resulted directly from hydrodynamic calculations or from the chosen steady-state. The obtained results are shown as graphs of $c_T^c(z)$ function.

Calculations were performed for the bioreactor with liquid internal loop and the following design dimensions: zone I and II height – $H_{\text{I}} = H_{\text{II}} = 1.75$ [m], zone I internal diameters – $d_{\text{I}} = 0.064$, 0.054 and 0.044 [m], zone II internal diameter – $d_{\text{II}} = 0.08$ [m]. These are the parameters of the reactor, for which the experimental verification of hydrodynamic model was described in earlier papers (Grzywacz, 2008, 2009).

2.3. Analysis of oxygen deficiency zones in the light of the choice of a mathematical model

A few conditions of reaction medium oxygenation can be distinguished for the process of aerobic biodegradation. The first condition refers to the situation, in which an intensive air barbotage provides so called sufficient medium oxygenation. In this case, the process can be described by single-substrate kinetics where carbonaceous substrate is the only limiting substrate. We say that such a formulated mathematical model belongs to the family of single-substrate models. If physical and chemical properties of the medium, the reactor construction or selection of the working parameters do not provide sufficient oxygenation, then we can speak about an extra limiting substrate in the process, namely oxygen dissolved in a liquid. In this case, the process is described by double-substrate kinetics. Thus the formulated mathematical model of the bioreactor belongs to the family of double-substrate models. The situation, in which life processes of bacteria present in the reactor result in total consumption of oxygen dissolved in the liquid, is also possible. In such a limiting case, anoxia, i.e. oxygen deficiency can occur leading to oxygen death of bacteria.

According to data published by Stamou, 1997, anoxia occurs if the concentration of oxygen dissolved in a liquid, c_T^c, falls below 5×10^{-4} [kg/m^3]. This phenomenon poses a risk of stopping biodegradation process. Lack of oxygen causes irreversible changes in metabolism, or even death of microorganisms. An increase in dissolved oxygen concentration after some time does not result in recovering the biological activity of bacteria. In the graphs demonstrated in this paper, the limiting concentration of dissolved oxygen, below which anoxia can arise, is defined as the Line of Limit Concentration for Anoxia – LCA.

The most favourite oxygenation conditions are related to the presence of gas phase in all zones of the reactor, namely in the hydrodynamic regime C. Therefore, at first, this operational state of the reactor was analysed. Calculations were made both for "plug flow" and dispersion flow in zones I and II. Simulations were performed for values of gas flow rate as low as possible, at which the reactor operates in regime C and for relatively high values of carbonaceous substrate concentration in the feed stream $c_{Af} = 0.2$ [kg/m^3]. High values of this concentration favour the occurrence of oxygen deficiency. The calculations were made for three values of volume distribution coefficient, i.e. $\zeta = 0.73$, 0.51 and 0.33. Results are presented in Figs. 2 and 3.

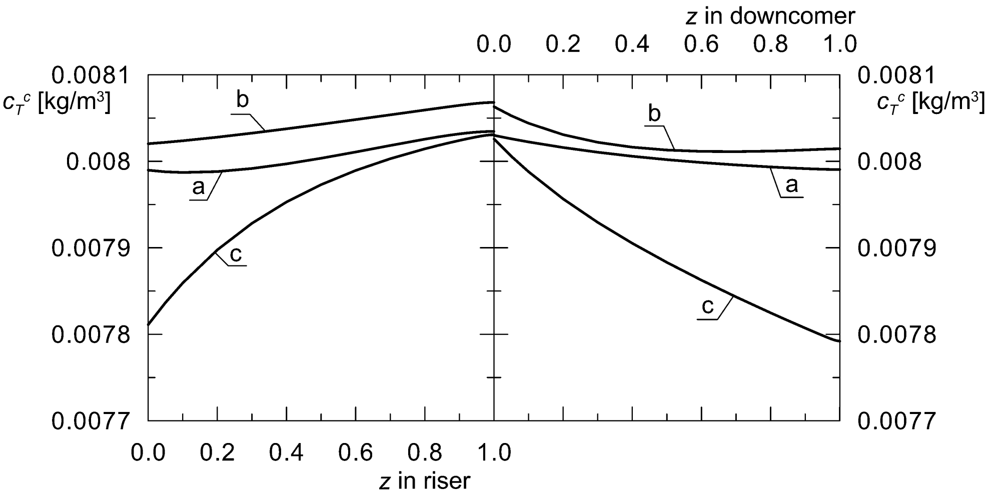

Fig. 2. Comparison of concentration of oxygen dissolved in liquid $c_T^c(z)$ obtained from model for hydrodynamic regime C for dispersion flow in zone I and II for three values of volume distribution coefficient $\zeta = 0.73$ (a), 0.51 (b) and 0.33 (c); $c_{Af} = 0.2$ [kg/m^3], $\tau_c = 10$ [h], $\tau_g = 0.013$ [h]

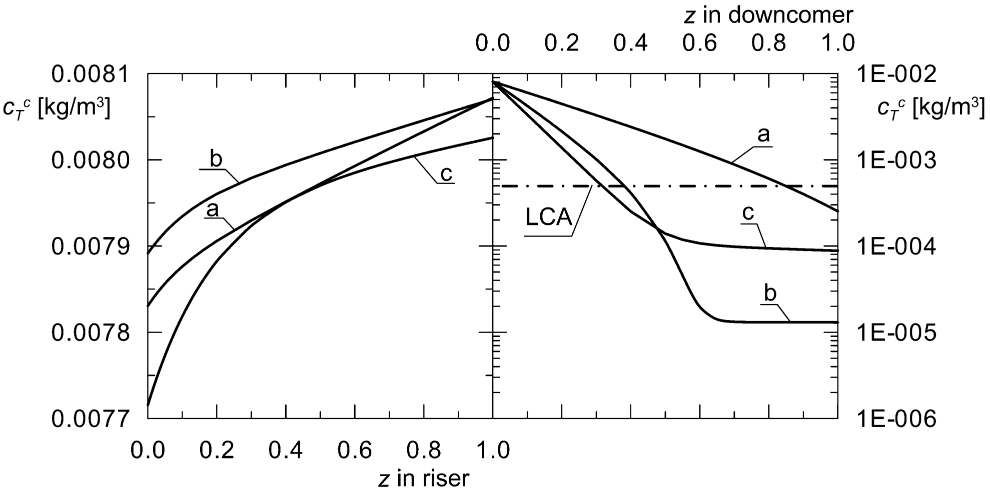

Fig. 3. Comparison of concentration of oxygen dissolved in liquid $c_T^c(z)$ obtained from model for hydrodynamic regime C for "plug flow" in zone I and II for three values of volume distribution coefficient $\zeta = 0.73$ (a), 0.51 (b) and 0.33 (c); $c_{Af} = 0.2$ [kg/m^3], $\tau_c = 10$ [h], $\tau_g = 0.013$ [h]; LCA – Line of Limit Concentration for Anoxia (Stamou, 1997)

The following conclusions can be drawn from the analysis of the charts. With the assumption that the fluid flows through the reactor in "plug flow", simulation results indicate that oxygen deficiency area may appear in the bioreactor. However, under the assumption of perfectly mixed fluid in the reactor the simulation revealed no areas of oxygen deficiency. Thus, the occurrence or absence of oxygen deficiency areas depends on the mathematical model chosen.

Subsequently, the effect of carbonaceous substrate concentration in the feed stream was tested. Calculations were performed for the bioreactor operating in the hydrodynamic regime A and for both analysed structures of media flows. Results are presented in Figs. 4 and 5. The performed calculations confirmed that high carbonaceous substrate concentration posed a risk of anoxia. This risk was detected regardless of the selected mathematical model describing the reactor.

The mean residence time of gas, that is a measure of intensity of bioreactor oxygenation, was the next parameter whose effect was analysed. The analysis was performed for both hydrodynamic regimes and

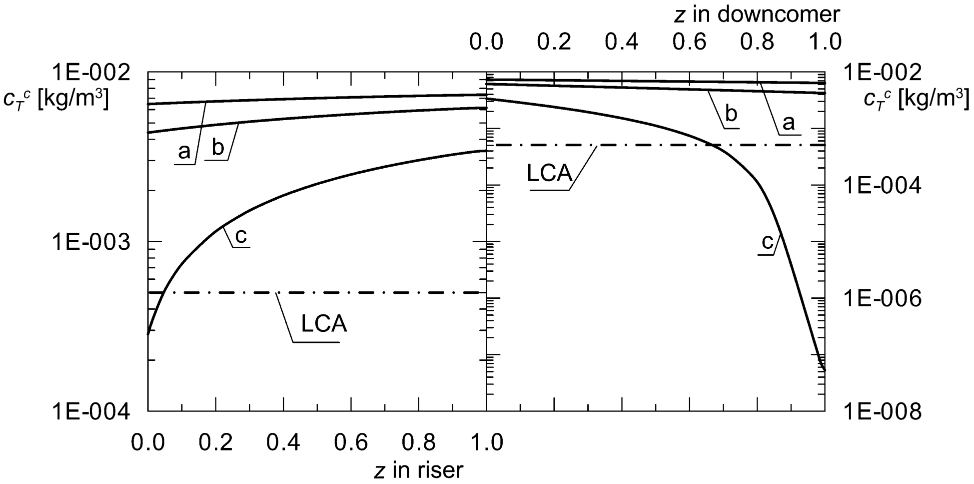

Fig. 4. Comparison of concentration of oxygen dissolved in liquid $c_T^c(z)$ obtained from model for hydrodynamic regime A for dispersion flow in zone I and II for three values of concentration of carbonaceous substrate at the inlet stream: $c_{Af} = 0.05$ (a), 0.1 (b), 0.2 (c) [kg/m^3]; $\zeta = 0.33$, $\tau_c = 10$ [h], $\tau_g = 0.0023$ [h]; LCA – Line of Limit Concentration for Anoxia (Stamou, 1997)

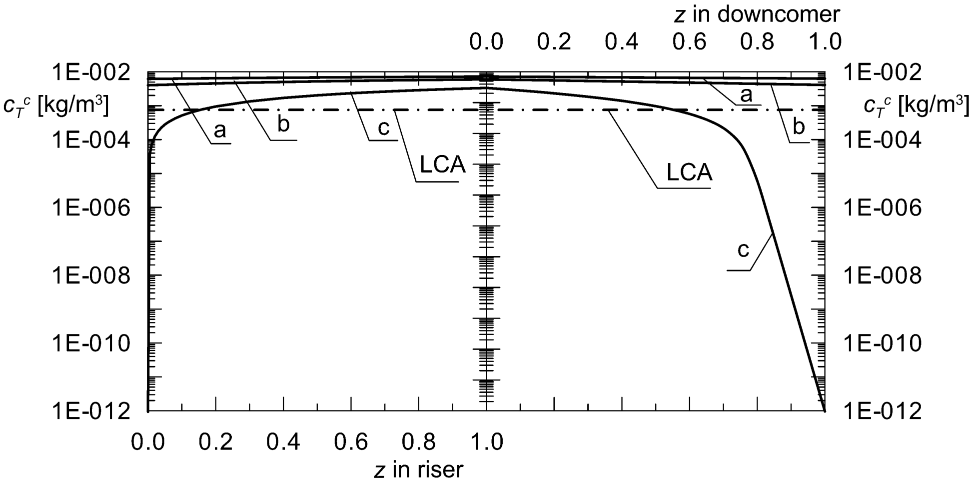

Fig. 5. Comparison of concentration of oxygen dissolved in liquid $c_T^c(z)$ obtained from model for hydrodynamic regime A for "plug flow" in zone I and II for three values of concentration of carbonaceous substrate at the inlet stream: $c_{Af} = 0.05$ (a), 0.1 (b), 0.2 (c) [kg/m^3]; $\zeta = 0.33$, $\tau_c = 10$ [h], $\tau_g = 0.0023$ [h]; LCA – Line of Limit Concentration for Anoxia (Stamou, 1997)

two volume partitioning coefficients ζ for "plug flow" and dispersion flow of media. Results are presented in Figs. 6–9. The calculations were made for carbonaceous substrate concentration in the feed stream $c_{Af} = 0.05$ [kg/m^3], that is the concentration found in wastewater if phenol is the substrate. The analysis of presented graphs shows that no oxygen deficiency is observed within the hydrodynamic regime C if this system can be described by dispersion flow. However, oxygen deficiency area occurs in a lower part of zone II if the existing conditions allow for assuming "plug flow" model. The analysis of the hydrodynamic regime A and low concentrations of carbonaceous substrate showed that no oxygen deficiency area was observed.

The mean residence time of liquid was the last parameter which effects oxygenation that was tested. Numerical simulation results are presented in Figs. 10 and 11. Calculations were performed for the hydrodynamic regime A and both analysed structures of media flow. As can be observed, reduced residence time of liquid in the reactor decreases the concentration of dissolved oxygen. However, this effect is insignificant and does not result in oxygen deficiency conditions for microorganisms.

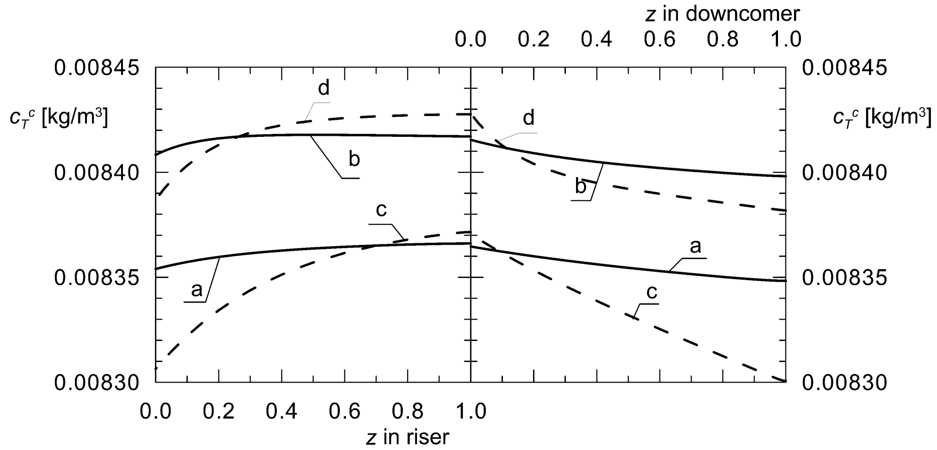

Fig. 6. Comparison of concentration of oxygen dissolved in liquid $c_T^c(z)$ obtained from model for hydrodynamic regime *C* for dispersion flow media in zone I and II for chosen values of volume distribution coefficient $\zeta = 0.73$ (——) and 0.33 (- - - -) and for two values total gas residence time: $\tau_g = 0.013$ (a and c), 0.003 (b and d) [h]; $c_{Af} = 0.05$ [kg/m^3], $\tau_c = 10$ [h]

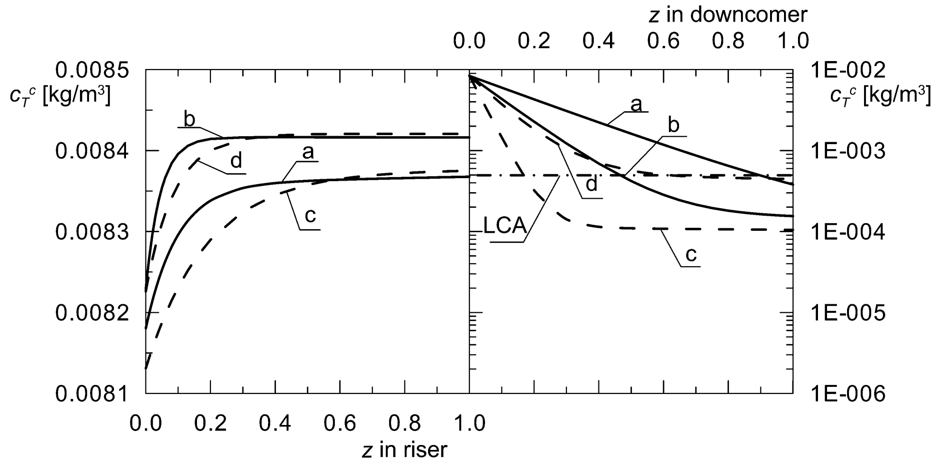

Fig. 7. Comparison of concentration of oxygen dissolved in liquid $c_T^c(z)$ obtained from model for hydrodynamic regime *C* for "plug flow" media in zone I and II for chosen values of volume distribution coefficient $\zeta = 0.73$ (——) and 0.33 (- - - -) and for two values total gas residence time: $\tau_g = 0.013$ (a and c), 0.003 (b and d) [h]; $c_{Af} = 0.05$ [kg/m^3], $\tau_c = 10$ [h]. LCA – Line of Limit Concentration for Anoxia (Stamou, 1997)

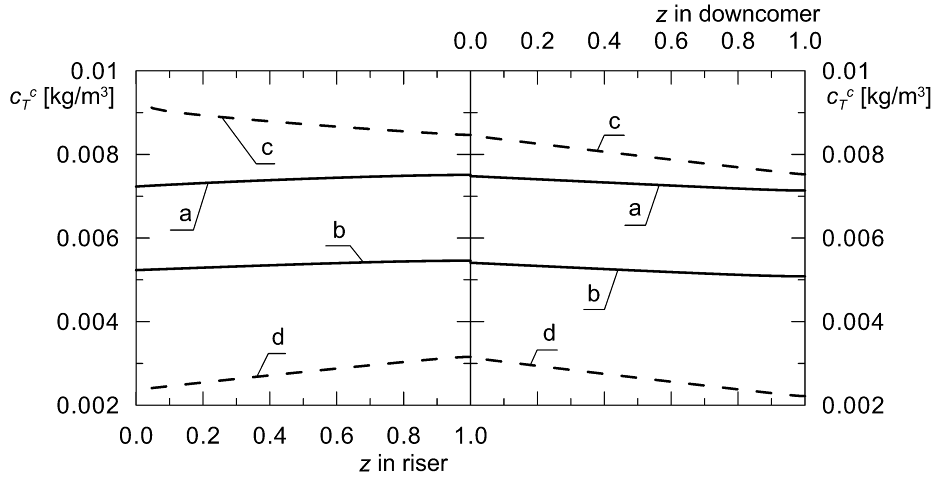

Fig. 8. Comparison of concentration of oxygen dissolved in liquid $c_T^c(z)$ obtained from model for hydrodynamic regime *A* for dispersion flow media in zone I and II for chosen values of volume distribution coefficient $\zeta = 0.73$ (——) and 0.33 (- - - -) and for two values total gas residence time: $\tau_g = 0.0015$ (a and c), 0.0005 (b and d) [h]; $c_{Af} = 0.05$ [kg/m^3], $\tau_c = 10$ [h]

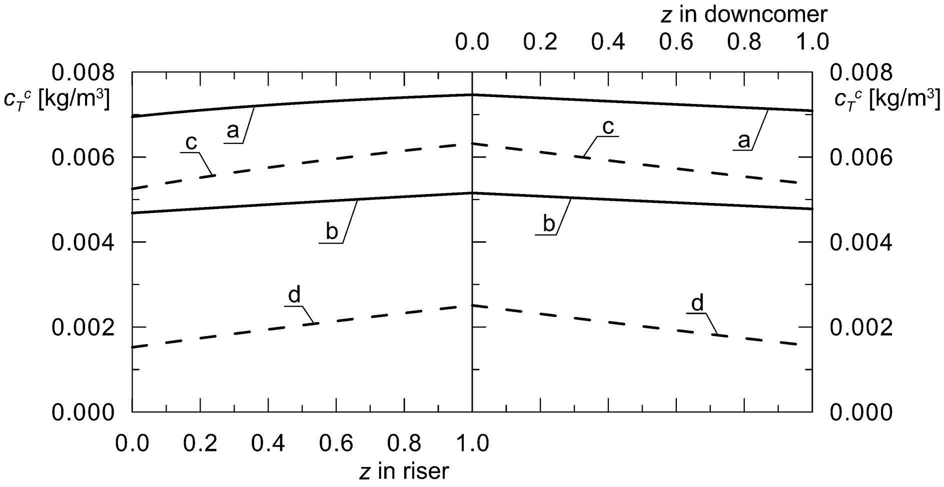

Fig. 9. Comparison of concentration of oxygen dissolved in liquid $c_T^c(z)$ obtained from model for hydrodynamic regime *A* for "plug flow" media in zone I and II for chosen values of volume distribution coefficient $\zeta = 0.73$ (——) and 0.33 (- - - -) and for two values total gas residence time: $\tau_g = 0.0015$ (a and c), 0.0005 (b and d) [h]; $c_{Af} = 0.05$ [kg/m³], $\tau_c = 10$ [h]

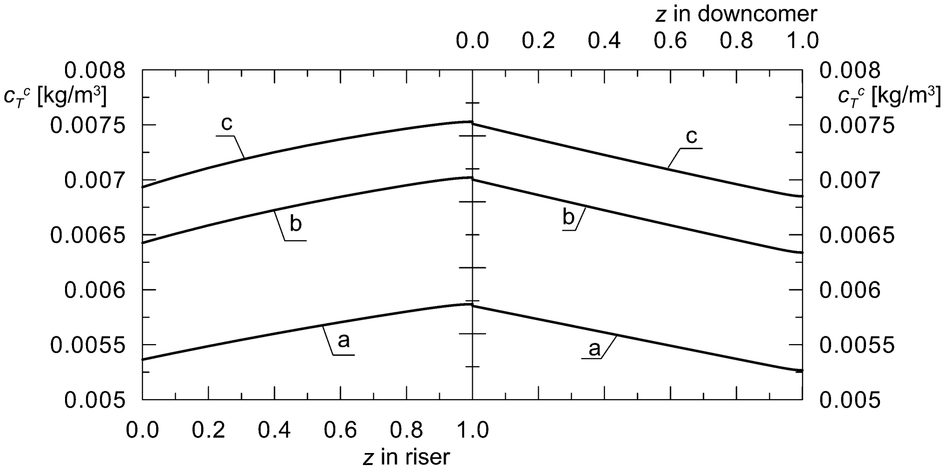

Fig. 10. Comparison of concentration of oxygen dissolved in liquid $c_T^c(z)$ obtained from model for hydrodynamic regime *A* for dispersion flow in zone I and II for chosen values total liquid residence time: $\tau_c = 5$ (a), 10 (b) and (c) [h]; $\zeta = 0.51$, $\tau_g = 0.0012$ [h]; $c_{Af} = 0.05$ [kg/m³]

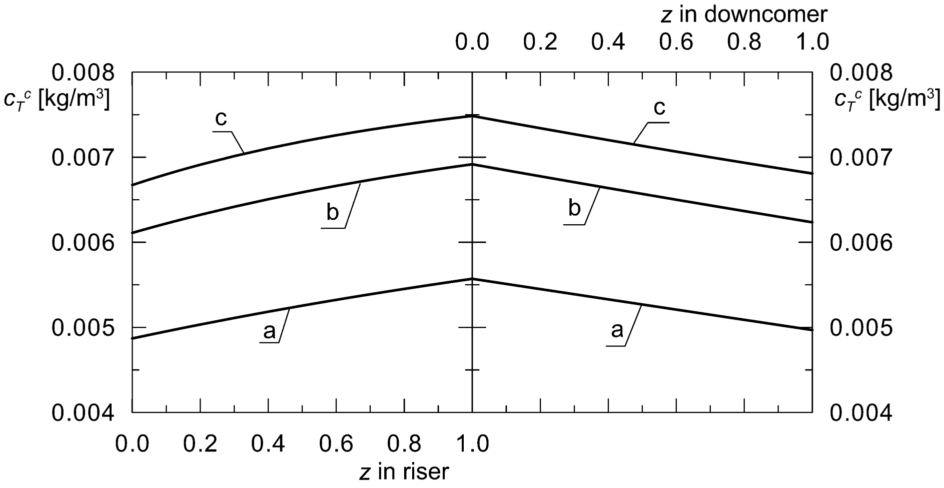

Fig. 11. Comparison of concentration of oxygen dissolved in liquid $c_T^c(z)$ obtained from model for hydrodynamic regime *A* for "plug flow" in zone I and II for chosen values total liquid residence time: $\tau_c = 5$ (a), 10 (b) and (c) [h]; $\zeta = 0.51$, $\tau_g = 0.0012$ [h]; $c_{Af} = 0.05$ [kg/m³]

3. CONCLUSIONS

- The mathematical models and the methods of their solutions presented in this paper, allow for a successful performance of computer simulations for the airlift bioreactor. Simulations can be performed for two most common hydrodynamic regimes, in which the analysed devices operate. The simulations enabled to draw conclusions about the reliable modelling and correct designing of the airlift reactors to avoid dangerous phenomena for the process, which are oxygen deficiency conditions for microorganisms.
- In the airlift bioreactors, anoxia may be related to different aspects. The hydrodynamic regime, in which the bioreactor operates, is the first aspect. The operational hydrodynamic regime depends on the reactor construction and the flow rate of supplied air. Airlift reactors with a liquid external loop usually operate in the hydrodynamic regime A. Thus, the lack of gas bubbles in zone II may result in the presence of anoxic conditions.
- If the bioreactor operates in the hydrodynamic regime C, the assumption of "plug flow" flow model for defining the media flow involves the presence of anoxic zones. However, the model does not predict the presence of anoxic zones if the dispersion flow is applied. Such a phenomenon does not occur even if very high values of the Péclet numbers are characteristic for the liquid flow.
- The volume of zone II affects the possibility of oxygen deficiency in simulation calculations. According to the calculations, anoxia occurs if the volume of zone II is equal to or higher than the volume of zone I. It is recommended to design airlift reactors with zone II significantly smaller than zone I. This reduces the liquid residence time in zone II that is in the area with the worse oxygenation conditions. This is particularly important for reactors with the external loop while reactors with the internal loop, with the lower volume of zone II in comparison with zone I, operate at lower values of gas flow in the hydrodynamic regime C. The presence of gas bubbles in zone II reduces the risk of oxygen deficiency.
- Insufficient intensity of oxygenation can be another reason for microorganisms anoxia. Simulation calculations show that too low gas flow rate, and therefore a large mean residence time of the gas, can result in anoxic conditions that are independent of hydrodynamic regime in which the reactor operates.
- It was observed that anoxia was related to excessive concentration of carbonaceous substrate. At high values of c_{Af}, deep minima of oxygen concentration are independent of gas phase flow rate. However, at low concentrations of carbonaceous substrate, the anoxic zone is related to the structure of media flow assumed. The model with plug flow predicts the occurrence of anoxic zones while the dispersion flow cannot do it, even at high values of the Péclet numbers. Thus the expectations of both models differ. The model with plug flow, which is easier for numerical application, at high values of the Péclet numbers poses a risk of incorrect interpretation of phenomena taking place in the bioreactor.
- The flow rate of the liquid phase, tied up with its mean residence time in the reactor, has the smallest effect on the possibility of anoxic zone presence. The reduction of the liquid residence time in the reactor slightly reduces the concentration of oxygen dissolved in liquid.
- Besides the process conclusions, the performed analysis shows another important conclusion related to modelling and simulation of the processes which take place in airlift bioreactors. The introduction of the assumption that the model with plug flow can replace the model with dispersion flow at high values of the Péclet numbers in the analysed bioreactor turned out to be incorrect.

SYMBOLS

ak_c, ak_{ci}	average and i-th zonal volumetric mass transfer coefficient [1/s]
c_{Ai}	mass concentration of carbonaceous substrate in i-th zone [kg/m^3]
c_{Bi}	mass concentration of biomass in i-th zone [kg/m^3]
c_{Ti}	mass concentration of oxygen dissolved in liquid in i-th zone [kg/m^3]
d_i	diameter of reactor i-th zone [m]

D_{mi}	dispersion coefficient in i-th zone [m^2/sec]
Fr	Froude number
F_{Vi}	volumetric flow rate in i-th zone [m^3/h]
g	gravitational constant [m^2/s]
h	current height [m]
H_i	height of i-th zone [m]
k, K_A, K_{in}, K_T	coefficients in kinetic equations
K_r	oxygen gas-liquid equilibrium constant [$\mathrm{m}^3_{\mathrm{liquid}}/\mathrm{m}^3_{\mathrm{air}}$]
k_{fi}	coefficient of flow resistance in i-th zone
Pe_i	Péclet number in i-th zone
$r_A,\ r_B,\ r_T$	reaction rate with reference to reagent A, B and T
S_i	cross-sectional area of i-th zone [m^2]
u_{ci}	velocity of liquid flow in i-th zone [m/s]
$u_{0c},\ u_{0g}$	specific velocity of liquid flow and specific velocity of gas flow [m/s]
V, V_i	total volume and volume of i-th zone [m^3]
$w_{BA},\ w_{BT}$	yield coefficients of biomass in relation to substrate A and T, subsequently
z	coordinate of dimensionless length of reactor

Greek

α_i	degree of conversion of carbonaceous substrate in i-th zone
β_i	dimensionless concentration of biomass in i-th zone
γ_i	dimensionless concentration of oxygen dissolved in liquid in i-th zone
δ_i	dimensionless concentration of oxygen in gas phase in i-th zone
ε_i	gas hold-up in i-th zone
ρ	density [kg/m^3]
$\tau,\ \tau_i$	total and mean residence time in i-th zone [h]
ξ	recirculation ratio
υ	slip velocity of gas bubbles
ζ	volume distribution coefficient

Indexes

I, II, III, IV	refer to the zone of a given number
A	refers to carbonaceous substrate
B	refers to biomass
T	refers to oxygen
c	refers to liquid phase
g	refers to gas phase
A, B, C	refer to hydrodynamic regime
i	i-th zone
f	refers to conditions at the inlet to the reactor
0	refers to conditions behind the mixing point

REFERENCES

Bales V., Antosova M., 1999. Mathematical and experimental modelling of phenol degradation in air-lift bioreactors. *Environ. Eng. Policy.*, 1, 209–216. DOI: 10.1007/s 100220050024.

Behin J., 2010. Modeling of modified airlift loop reactor with a concentric double-draft tube. *Chem. Eng. Res. Des.*, 88, 919–927. DOI: 10.1016/j.cherd.2010.01.004.

Boyadjiev Ch., 2006. On the modeling of an airlift reactor. *Int. J. Heat Mass Transfer*, 49, 2053–2057. DOI: 10.1016/j.ijheatmasstransfer.2006.01.015.

Camarasa E., Carvalho E., Meleiro L.A.C., Maciel Filhob R., Domingues A., Wild G., Poncin S., Midoux N., Bouillard J., 2001. Development of a complete model for an air-lift reactor. *Chem. Eng. Sci.*, 56, 493–502. DOI: 10.1016/S0009-2509(00)00253-0.

Chisti Y., 1989. *Airlift bioreactors*. Elsevier, London.

Gavrilescu M., Tudose R.Z, 1998. Concentric-tube airlift bioreactors. Part I: Effects of geometry on gas holdup. *Bioproc. Eng.*, 19, 37–44. DOI: 10.1007/s004490050480.

Grzywacz R., 2003. The methods of the determining the steady-states of an airlift bioreactor for selected hydrodynamic structures of the liquid phase. *Inż. Chem. Proc.*, 24, 567–587.

Grzywacz R., 2008. Experimental verification of hydrodynamic models for airlift reactor. *Technical Journal – Mechanics*. *Cracow University of Technology*, (105) M–5, 151–158.

Grzywacz R., 2009. Influence of construction and process parameters on gas holdup coefficient in downcomer of airlift reactor. *Inż. Ap. Chem.*, 48, 76–78.

Grzywacz R., 2012a. Continuous mathematical models of airlift bioreactors: Families, affinity, diversity and modelling for single-substrate kinetics. *Chem. Process Eng.*, 33, 291–309. DOI: 10.2478/v10176-012-0027-9.

Grzywacz R., 2012b. *Steady-state properties of airlift bioreactors*. Wydawnictwo PK, Kraków.

Kanai T., Ichikawa J., Yoshikawa H., Kawase Y., 2000. Dynamic modeling and simulation of continuous airlift bioreactors. *Bioproc. Eng.*, 23, 213–220. DOI: 10.1007/s004499900154.

Kanai T., Uzumaki T., Kawase Y., 1996. Simulation of airlift bioreactors: steady-state performance of continuous culture processes. *Comp. Chem. Eng.*, 20, 1089–1099. DOI: 10.1016/0098-1354(95)00225-1.

Korpijarvi J., Oinas P., Reunanen J., 1999. Hydrodynamics and mass transfer in an airlift reactor. *Chem. Eng. Sci.*, 54, 2255–2262. DOI: 10.1016/S0009-2509(98)00439-4.

Merchuk J.C., Stein Y., 1980. Distributed parameter model of an airlift fermentor. *Biotechnol. Bioeng.*, 22, 1189–1211. DOI: 10.1002/bit.260220607.

Sanchez A., Ceron Garcia C., Garcia Camacho F., Molina Grima E., Chisti Y., 2004. Mixing in bubble column and airlift reactors. *Chem. Eng. Res. Des.*, 82, 1367–1374. DOI: 10.1205/cerd.82.10.1367.46742.

Seker S., Beyenal H., Salih B., Tanyolac A., 1997. Multi-substrate growth kinetics of pseudomonas putida for phenol removal. *Appl. Microbial. Biotechnol.*, 47, 610-614. DOI: 10.1007/s002530050982.

Sikula I., Markoš J., 2008. Modeling of enzymatic reaction in an airlift reactor using an axial dispersion model. *Chem. Pap. - Chem. Zvesti*, 62, 10–17. DOI: 10.2478/sl1696-007-0073-9.

Stamou A., 1997. Modelling of oxidation ditches using an open channel flow 1-D advection-dispersion equation and ASM1 process description. *Wat. Sci. Tech.*, 36/5, 269–276. DOI: 10.1016/S0273-1223(97)00483-6.

Tabiś B., Grzywacz R., 2011. Numerical and technological properties of bubble column bioreactors for aerobic processes. *Comp. Chem. Eng.*, 35, 212–219. DOI: 10.1016/j.compchemeng.2010.03.015.

Towell G., Ackerman G., 1972. Axial mixing of liquid and gas in large bubble reactors. *Proceedings of the 5th European/ 2nd International Symposium Chemical Reactor Engineering*, Amsterdam. B3 1–13.

Vial Ch., Poncin S., Wild G., Midoux N., 2001. A simple method for regime identification and flow characterization in bubble columns and airlift reactors. *Chem. Eng. Proc.*, 40, 135–151. DOI: 10.1016/S0255-2701(00)00133-1.

Wisecarver K., Fan L., 1989. Biological phenol degradation in a gas-liquid-solid fluidized bed reactor. *Biotech. Bioeng.*, 33, 1029–1038. DOI: 10.1002/bit.260330812.

Znad H., Báleš V., Markoš J., Kawase Y., 2004. Modeling and simulation of airlift bioreactors. *Biochem. Eng. Journal.*, 21, 73–81. DOI: 10.1016/j.bej.2004.05.005.

Received 19 June 2017
Received in revised form 11 June 2018
Accepted 30 October 2018